Plasma Science and Technology

PAPER

Effects of temperature on creepage discharge characteristics in oil-impregnated pressboard insulation under combined AC–DC voltage

Plasma Sci. Technol. **21** (2019) 054002 (9pp) https://doi.org/10.1088/2058-6272/aaff01

Effects of temperature on creepage discharge characteristics in oil-impregnated pressboard insulation under combined AC–DC voltage

Fubao JIN (金福宝)[1], **Yuanxiang ZHOU** (周远翔)[2], **Bin LIANG** (梁斌)[1], **Zhongliu ZHOU** (周仲柳)[2] **and Ling ZHANG** (张灵)[2]

[1] Key Laboratory of Plateau Ecology and Agriculture, College of Agriculture and Animal Husbandry, School of Water Resources and Electric Power, Qinghai University, Xining 800016, People's Republic of China
[2] State Key Lab of Control and Simulation of Power Systems and Generation Equipments, Department of Electrical Engineering, Tsinghua University, Beijing 100084, People's Republic of China

E-mail: jinfubao@163.com

Received 19 September 2018, revised 15 January 2019
Accepted for publication 16 January 2019
Published 1 March 2019

Abstract

Due to the complexity of the valve side winding voltage of the converter transformer, the insulation characteristics of the oil-impregnated pressboard (OIP) of the converter transformer are different from those of the traditional AC transformer. The study on effect of temperature on the creeping discharge characteristics of OIP under combined AC–DC voltage is seriously inadequate. Therefore, this paper investigates the characteristics of OIP creepage discharge under combined AC–DC voltage and discusses the influence of temperature on creepage discharge characteristics under different temperatures from 70 °C to 110 °C. The experimental results show that the partial discharge inception voltage and flashover voltage decrease with increasing temperature. The times of low amplitude discharge (LAD) decrease and amplitude of LAD increases. Simultaneously, the times of high amplitude discharge (HAD) gradually increase at each stage of creepage discharge with higher temperature. The analysis indicates that the charge carriers easily accumulate and quickly migrate directional movement along the electric field ahead of discharging. The residual charge carriers are more easily dissipated after discharging. The 'hump' region of LAD moves to the direction of higher discharge magnitude. The interval time between two continuous discharges is shortened obviously. The concentration of HAD accelerates the development of OIP insulation creepage discharge. The temperature had an accelerating effect on the development of discharge in the OIP under applying voltage.

Keywords: oil-impregnated pressboard insulation, combined AC–DC voltage, inception voltage, creepage discharge, temperature, flashover voltage

(Some figures may appear in colour only in the online journal)

1. Introduction

The transmission voltage of ultra high voltage direct current (UHVDC) system has been continuously raised from ±800 kV to ±1100 kV in China. As a core equipment of UHVDC transmission system, the oil-impregnated pressboard (OIP) insulation of converter transformers will face more severe challenges not only by the complex insulation structure and operating condition but also by multi-field stress—DC, AC (50 Hz) and combined AC–DC voltage, especially outlet device in the valve winding [1, 2]. The temperature of OIP will be increased due to the effect of Joule heating and stray losses under different loads in the converter transformer. However, the distribution of DC electric field is directly

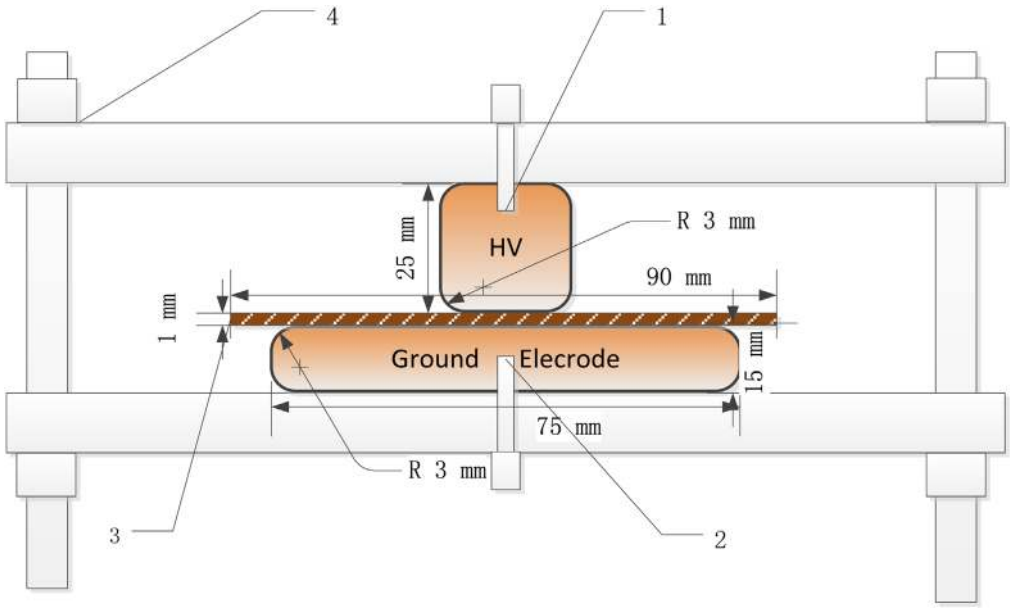

Figure 1. Cylindrical-plate electrode configuration (1: high voltage electrode, 2: ground electrode, 3: OIP, 4: polytetrafluoroethylene. The pressboard thickness was 1 mm).

proportional to the conductivity of oil and pressboard. But because the conductivity of OIP is much lower than that of transformer oil. The electric field mainly concentrates on OIP under DC voltage. However, the conductivity of OIP is affected by humidity, impurity, temperature and electric field [3, 4]. So the distribution of electric field and the discharge characteristics of OIP are influenced by these factors.

The phenomenon of creepage discharge in OIP is attracted attention widely at home and abroad. Previous studies have focused on the discharge location, strength, mechanism, and streamer characteristics of creepage discharge under single voltage type, such as AC, DC and impulse voltage [5–10]. Kenneth Wechsle *et al* discussed the creepage discharge characteristics in the several insulating materials under AC (60 Hz) and impulse voltage. The results show that the flashover voltage can be effectively increased by matching the dielectric constant of solid–liquid insulation [11–14]. H Okubo *et al* studied the creepage discharge in the OIP under lighting impulse voltage. The influence of electric field distribution and oil volume on the flashover voltage on the surface of high voltage electrode was analyzed in 1987 [15]. M R Raghuveer *et al* compared the creepage discharge characteristics of OIP under pure AC, pure DC, and combined AC–DC voltage in 1990 [16]. S S Tulasi Ram investigated the flashover voltage of OIP insulation under combined voltage in 1994 [17]. The effect of temperature on creepage discharge of OIP at AC voltage was studied by Li Chengrong. The experimental result showed that the flashover voltage decreased along with higher temperature in 2010 [18].

The temperature rise limit of a power transformer is determined according to different load conditions, which is according to the IEC 76.2-1993. According to the rated capacity, the standard ambient temperature of the oil-immersed transformer is 40 °C, and the oil temperature at the top of the transformer usually does not exceed 95 °C. Meanwhile, the level A insulating materials standing highest temperature is 105 °C. Since the flash point temperature of the 25# transformer oil is 140 °C, the operating temperature of the power transformer is 70 °C to 90 °C. Therefore, the effect of temperature on the creepage discharge characteristics under combined AC–DC voltage was studied at 70 °C to 110 °C.

Researchers have studied the space charge characteristics, discharge characteristics, and diffusion characteristics of OIP insulation under different voltage types, such as DC, AC, and polarity reversal [19–25]. At the same time, the effects of temperature, moisture and other parameters on the electrical properties of OIP insulation were studied, and some research results were also obtained [26–32]. But they did not pay more attention to creepage discharge characteristics in OIP under combined AC–DC voltage due to shorter operating time. Therefore, the effect of temperature on the discharge characteristics of OIP insulation materials under combined AC–DC voltage is studied in this study, and the partial discharge (PD) signals in the whole discharge process are calculated. The influence of different temperature and electric field on the development of creepage discharge of OIP insulation is analyzed, and the discharge characteristics of each stage in the whole development process of creepage discharge are analyzed. The effect of temperature on surface discharge characteristics of OIP insulation is revealed. The results are of great significance for understanding the development process of creepage discharge and judging the severity of creepage discharge development in converter transformer.

2. Experimental device

2.1. Samples preparation

The transformer oil used in the UHVDC converter transformer was Karamay 25# oil. According to GB2536.90 (EQV

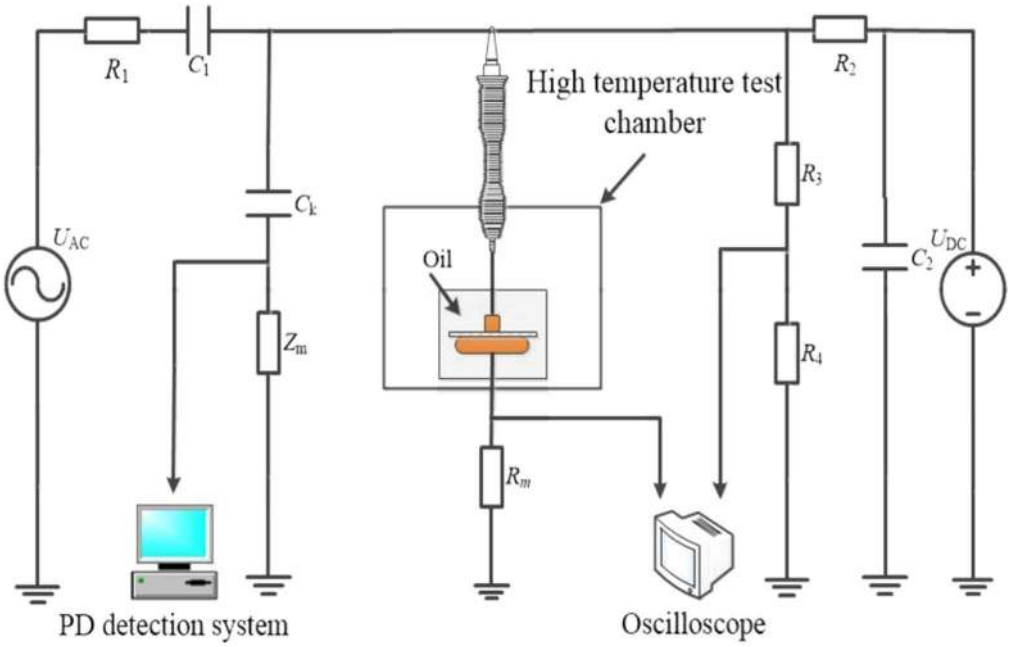

Figure 2. Diagram of experimental system. $R_1 = 10$ MΩ, $R_2 = 1$ MΩ, R_3/R_4: resistive voltage divider (10000:1), $R_m = 5$ MΩ, and $C_1 = 0.2$ μF, $C_k = 400$ pF 1: PD detection system, 2: digitizer oscilloscope.

IEC 296-82), the transformer oil was filtered by the vacuum filter device to realize vacuum degassing and dehumidification treatment of the transformer oil. After treatment, the moisture content in transformer oil was not more than 5 ppm, and the gas content was not more than 2% [33–36].

The pressboard thickness was 1 mm and the area was 90 mm × 90 mm. The insulating pressboard was dried in a hot air oven at 105 °C for 72 h, then vacuum dried at 85 °C for 48 h, and finally immersed at room temperature for 72 h with a vacuum apparatus. The purpose of this process is to control the moisture level of the fully impregnated pressboard sample to a weight of about 0.3%. In order to improve the reliability of the experiment, all the samples used in the test were composed of the above-mentioned sample oil and pressboard [33–36].

2.2. Electrode composition

The experimental electrode configuration was used to investigate the effect of temperature on creepage discharge characteristics, as shown in figure 1. The whole electrode was made of stainless steel and designed according to CIGRE Method II. The cylinder electrode diameter was 25 mm × 25 mm, and the plane diameter was 75 mm. The pressboard sample was 1 mm thick with size of 90 mm × 90 mm. As shown in figure 1, in order to ensure close contact between the electrode and pressboard, a polytetrafluoroethylene was used to tighten electrode configuration, thereby reducing the experimental error [33–36].

2.3. Experimental system

Figure 2 shows the experimental arrangement allowing PD detection under combined AC–DC voltage. Figure 2 shows a block diagram of an experimental system for PD detection under combined AC–DC voltage. As shown in figure 2, the U_{DC} is a 100 kV DC voltage source that is connected to the detection circuit using current-limiting resistance R_2. U_{AC} is a 100 kV AC voltage source that is connected to the detection circuit using current-limiting resistance R_1 and blocking capacitor C_1. The PD detection system used pulse current method to detect PD signal. The experimental device was used to record flashover voltages. The bandwidth of the PD measurement device is 0.04–1 MHz, which provides enough information for the measurement of PD signals measurements. When there is no pressboard sample, the experimental system can maintain at least 70 kV without PD signal [33–36].

2.4. Voltage application method

In the creepage characteristic test of OIP insulation under combined AC–DC voltage, the voltage is increased at a rate of 1 kV s^{-1} until a breakdown voltage (U_b) of 20% is reached, and then the voltage is gradually increased (2 kV per step). As shown in figure 3, the DC voltage is raised to a predetermined value for 5 min, and then the AC voltage is gradually increased to form combined AC–DC voltage. The voltage is gradually increased until the PD signal appears. The present voltage was defined as PD inception voltage (PDIV). Then the voltage is raised continually until 100 pC emerges and remains until flashover happens. The present voltage was defined as creepage discharge voltage (CDFV). The main reason for choosing this application method is to consider the effect of conduction current on creepage discharge. During the charge carrier migration process, with the generation, injection and recombination of charge carriers, the current gradually decreases during the polarization process and tends

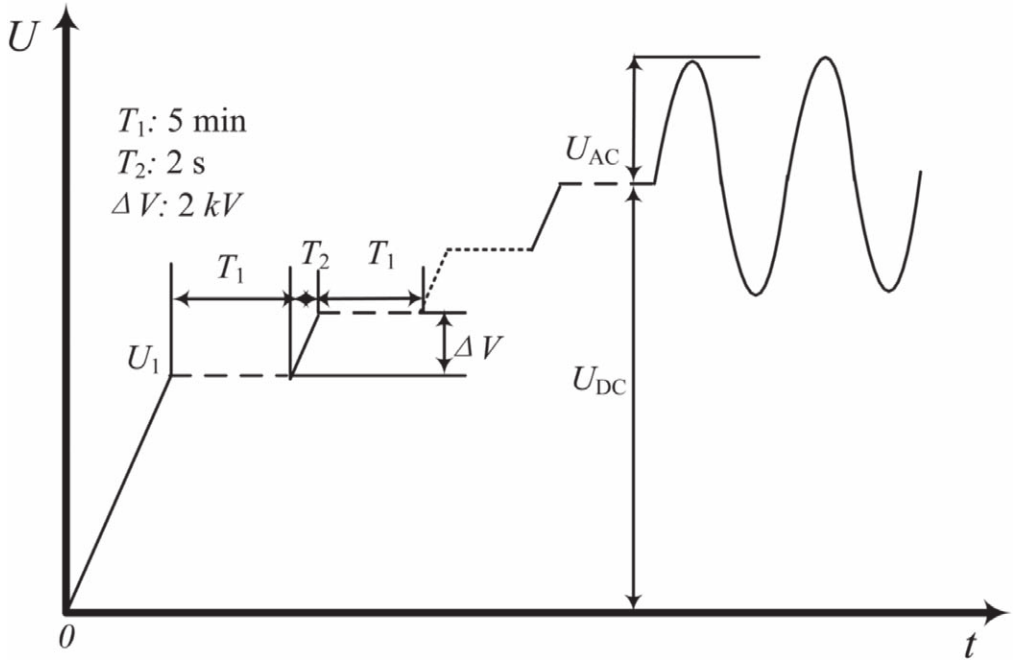

Figure 3. Application method of combined AC–DC voltage. ($U_1 = 20\%U_b$, U_b is the breakdown voltage of 1 mm OIP (42 kV), U_{AC} is AC voltage component, U_{DC} is DC voltage component).

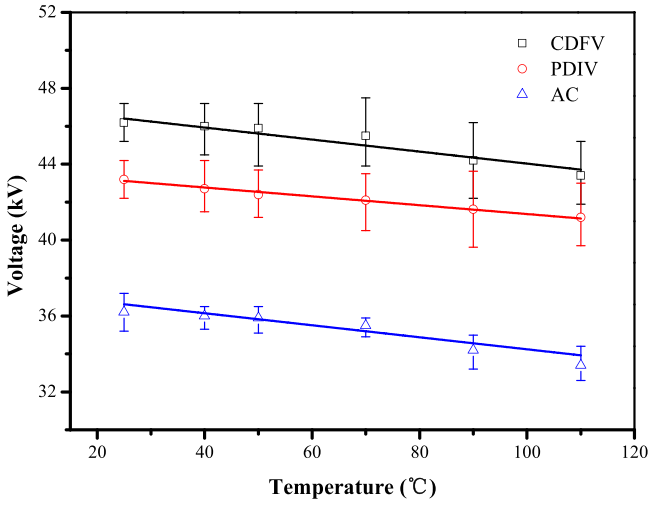

Figure 4. PDIV and CDFV under different temperatures (DC voltage component 10 kV).

to be stable at constant amperage for about 5 min [33–36]. Usually, 10 repeated tests will be performed at each temperature.

3. Results and discussion

3.1. Effect of temperature on inception voltage and flashover voltage of creepage discharge

Compared with the PD characteristics under AC voltage, the OIP insulation under the combined AC–DC voltage shows a great difference. The PD signal under combined AC–DC voltage is a random discharge pulse, which is not periodic as the AC PD signal. It is difficult to determine PDIV according to the provisions in IEC 60270 [37, 38]. In this study, PDIV under combined AC–DC voltage is defined as the average voltage of multiple voltage measurements in which the first discharge pulse is detected in the pressboard sample.

As shown in figure 4, PDIV and CDFV gradually decrease with the increase of test temperature under the combined AC–DC voltage. The impurity ions were activated due to thermal excitation by the higher temperature in the oil and OIP, and they formed ionic conductivity through directional thermal transit. As the temperature increasing, the resistivity of the transformer oil and OIP will decrease. The amount of impurity would increase and move quickly. Therefore, the PD could easily occur under lower voltage due to higher temperature. Therefore, the AC voltage component displayed a decreasing trend with higher temperature.

3.2. The characteristic spectrum of creepage discharge under different temperatures

The PD signals were detected and captured by the PD measurement during the whole creepage discharge process under applied voltage. Then the characteristics spectrums at different stages of creepage discharge were extracted from the PD signals. These PD characteristic spectra could reflect the creepage discharge trend of OIP at different temperatures under the combined AC–DC voltage. However, the PD signal under combined AC–DC voltage was a random discharge pulse, which was not periodic as the AC PD signal. Therefore, the interval time Δt between adjacent discharges is used to replace the concept of phase φ in the conventional AC. Δt is

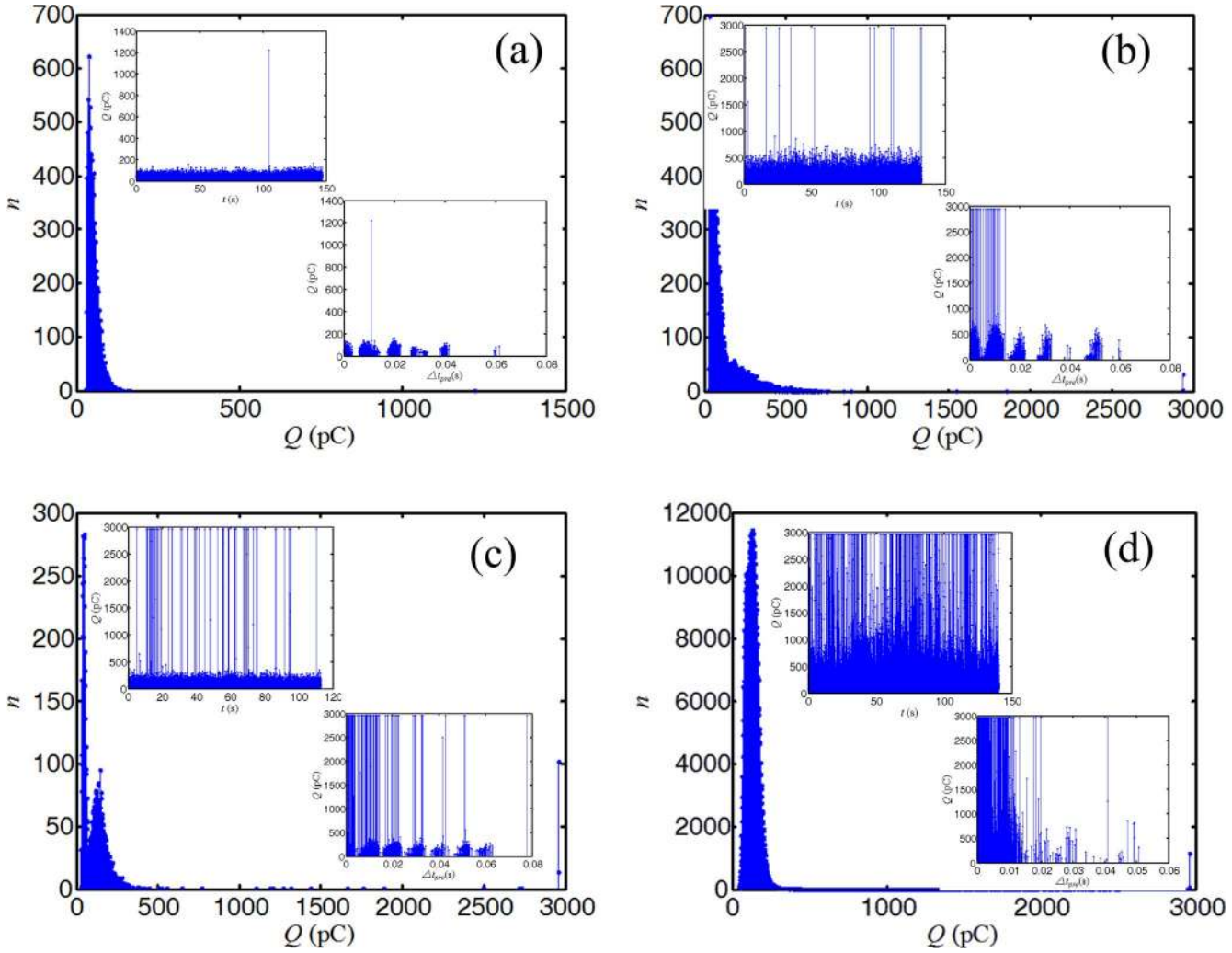

Figure 5. Creepage discharge characteristic spectra in OIP under combined AC–DC voltage at 70 °C (AC 35.5 kV, DC 10 kV).

the time interval Δt_{pre} between the current discharge pulse and the previous discharge pulse. The interval time Δt is combined with the traditional characteristic parameter discharge magnitude Q and the number of discharges n to form different statistical characteristic spectra. The time resolved pulse sequence analysis is used to reflect the different discharge processes in the study. The time domain distribution spectra of the discharge phase can more easily judge the change process of the creepage discharge development. Because the pulse sequence distribution pattern contains too much information, the dimensionality of the data with high dimensionality is reduced, some characteristic spectra are obtained, and the characteristic parameters are extracted to analyze the discharge development process.

Therefore, three important parameters of discharge magnitude Q, discharge number n and discharge interval time Δt are selected in the study to form a PD characteristic spectrum. Q–t reflects the relationship between the discharge magnitude and the discharge time. Δt_{pre}–Q reflects the relationship between the interval time between adjacent discharges and the discharge magnitude. By analyzing the statistical rule of the spectrums, the influence of temperature on the development process of the creepage discharge can be better reflected, which can effectively reflect the relationship between the change in material defects and the discharge magnitude of discharge development. Q–n spectrum can statistically analyze the relationship between the discharge magnitude and the number of discharges during the development of the creepage discharge, and then provide a basis for the different stages of the development process of the creepage discharge. Q–t, Q–n, Δt_{pre}–Q show the different stages of the development of creepage discharge in OIP insulation under different temperatures and electric field types. The above three spectra are displayed in one figure for display, which can more intuitively reflect the trend of three parameters of creepage discharge, and can also better reflect the development trend of creepage discharge [33–36].

As shown in figure 5, the development of creepage discharge was divided into four stages according to the statistical characteristics of creepage discharge signal under combined AC–DC voltage. The characteristic spectra of creepage discharge at 70 °C under combined AC–DC voltage were analyzed in this section. The DC voltage component was 10 kV, and the AC voltage component was 35.5 kV.

Figure 5 shows the characteristic spectra of OIP insulation creepage discharge at 70 °C combined AC–DC voltage. At initial stage, the amplitudes of discharges were relatively smaller and most of discharge magnitudes were concentrated in range of 10–170 pC (the background noise of measurement was less than 10 pC). The number of discharge was more than 600 times. But the high amplitude discharge (HAD 2596 pC) occasionally occurred during the initial stage, but the number of it was very few. The Δt_{pre} was relatively evenly distributed over the entire range of 0–0.04 s. The discharge magnitude was mainly dominated by the low amplitude discharge (LAD) at the initial stage in the *Q*–*t*. The discharge magnitude relatively went up and most of discharge magnitude were concentrated in range of 10–300 pC. The HAD appeared more times than the initial stage, which went up to 30 times. The Δt_{pre} of HAD was distributed over 0–0.01 s and the amplitude discharge raised up in this time interval range. The Δt_{pre} of LAD was distributed over 0.02–0.06 s. At the third stage, the amplitude of LAD went up to 10–350 pC. The HAD appeared more than 100 times.

The Δt_{pre} of HAD was distributed over 0–0.02 s. The amplitude of LAD went up to 10–450 pC at the last stage of creepage discharge, and the times of LAD approached to 12 000. Meanwhile, the HAD went up to 1700 times. The Δt_{pre} almost occupied the range of 0–0.01 s and appeared intermittently within 0.02–0.04 s. The performance of OIP became worse, resulting in a higher discharge repetition rate. The discharge which was distributed over 0.02–0.04 s presented a decreasing trend. The HAD intensively appeared at this stage. Therefore, the defects within insulating material become more serious, the insulating effect was substantially lost, and eventually high magnitude discharge pulse appeared.

It could be seen that many LAD always followed after the HAD happening in the *Q*–*t*. It indicated that the residual charge would move rapidly along the direction of the electric field, causing a neutralization discharge to form LAD. The energy dissipated by the HAD resulted in decomposing the oil and OIP. Some decomposition products were formed and dissolved or floated in the oil and OIP. Figure 5 depicted the creepage discharge characteristics under each stage during entire process under 70 °C. It could be concluded that the shape of LAD appeared in 'hump form' at each stage of creepage discharge in *Q*–*n*, and the times of HAD gradually increased under different stages.

The experimental results show that the discharge amplitude and interval time are different in each stage of the creepage discharge in figure 5. Meanwhile, the trendency of characteristic spectra under different temperature was similar to that under 70 °C. But the discharge magnitude gradually increased at each stage under different temperatures from 70 °C to 110 °C. The interval time between two consecutive discharges gradually shorten with higher temperature. In this section, the fourth stage of creepage discharge spectra *Q*–*n* was discussed under different temperatures from 70 °C to 110 °C, as shown in figure 6.

The experimental results showed that the n_2 (n_2 is times of LAD (⩾2900 pC)) of HAD drastically increased with higher temperature. It increased from 600 under 70 °C to 2.5 × 10^5 under 110 °C. Because the n_2 of HAD under 110 °C was far greater than that under 70 °C–90 °C. So the tendency of discharge magnitude under 110 °C was intercepted from 0 to 1700 pC. The n_1 (n_1 is times of LAD (<2900 pC)) of LAD gradually decreased from 11 500 to 1000 with higher temperature. Meanwhile, the amplitude of LAD gradually increased with higher temperature.

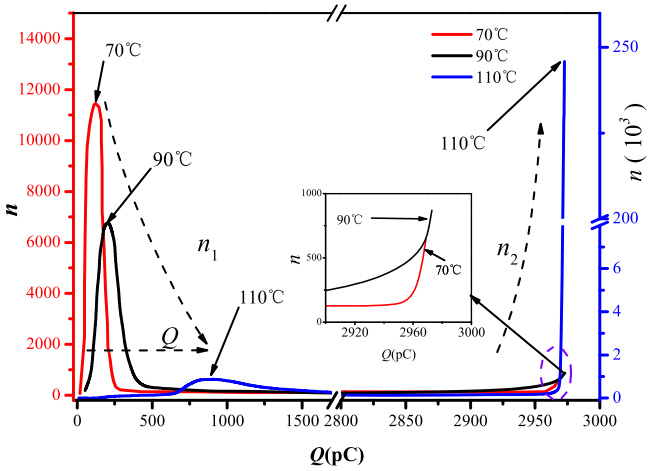

Figure 6. The fourth stage of creepage discharge under different temperatures (n_1 is times of LAD (<2900 pC), n_2 is times of LAD (⩾2900 pC)).

The amplitude of LAD was moving to right along the direction of higher discharge magnitude, as shown in figure 6 by the arrows. The range of discharge magnitude under hump area increased from 170–240 pC under 70 °C to 700–1600 pC under 110 °C. Thus, the n_1 of LAD gradually decreased, and the n_2 of HAD drastically increased with higher temperature in the OIP under the same combined AC–DC voltage. The amplitude of LAD gradually increased with higher temperature. The results show that temperature can promote the development of OIP creepage discharge, especially in increasing the discharge amplitude.

As the temperature increased, the volume and surface conductivity of the OIP insulation gradually increased, and the molecular dissociation activation energy decreased. These factors accelerated the generation and the dissociation, migration and recombination reactions of carriers in the OIP insulation under combined AC–DC electric field. At the same time, under the same electric field, the density and total amount of space charge injected into the OIP insulation also increased with the increasing temperature. This caused the field strength distortion to increase, and the space charge balance state was more susceptible to disturbance. As temperature raised, the equilibrium state was destroyed, causing the trapped charge to collapse into a free charge. The free charge moved continuously with the change of temperature. As the temperature increased, the rate of electron migration and accumulation increased. Meanwhile, the depolarizing energy caused the surrounding trapped charge to be released like an avalanche. Meanwhile, as the temperature increased, part of the charge in the paper diffused into the oil, causing the field strength in the oil to increase. When the electric field strength was sufficient to cause oil breakdown, a large amount

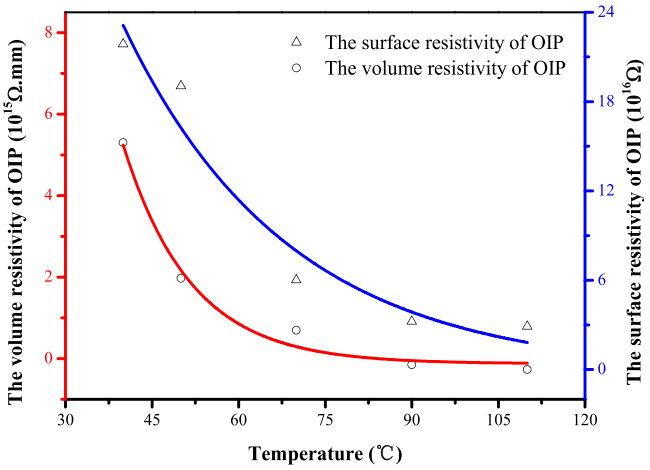

Figure 7. Surface and volume resistivity of 1 mm OIP under different temperatures. (DC electric field strength 1 kV mm^{-1}).

of electric charge accumulated instantaneously, thereby forming large amplitude discharge while accelerating the dissipation rate of space charge in the OIP insulation. Based on the above two reasons, the discharge amplitude Q increased as temperature increases during the creeping discharge, and the times n_1 of the small amplitude discharge decreased.

The phenomenon that the times n_1 of LAD gradually decreased, and the times n_2 of HAD drastically increased with higher temperature had a close relationship with the conductivity of OIP. On one hand, the degree of dissociation gradually increased with higher temperature, on the other hand, the ions were more easily getting enough energy to go over potential barrier region to free ions as the temperature was raised. Therefore, as shown in figure 7, the volume and surface conductivity of 1 mm thick OIP insulation at different temperatures at 1 kV mm^{-1} DC have been measured.

Figure 7 illustrated the relationship between temperature and volume and surface resistivity of OIP. The results indicated that the surface and volume resistivity of OIP decreased exponentially with higher temperature. The fitting equation of volume resistivity of OIP was $\rho_v = 2.09 \times 10^{15} + 2.9 \times 10^{18}e^{-0.08T}$, where ρ_v is volume resistivity of OIP (unit: Ω mm) and T is temperature (unit: °C). The volume resistivity of OIP decreased two order of magnitude from 40 to 110 °C, resulting in conduction current increasing in the OIP, the temperature increasing. The surface resistivity of OIP decreased one order of magnitude from 40 °C to 110 °C. The fitting equation of surface conductivity of OIP was $\rho_s = 3.13 \times 10^{16}e^{-0.033T}$–$9.6 \times 10^{14}$, ρ_s is surface conductivity of OIP (unit: Ω) and T is temperature (unit: °C). Thus, the creepage discharge was more easily developing along the surface of OIP under combined AC–DC voltage. Meanwhile, the resistivity of oil and OIP was seriously influenced by the temperature. The surface and volume resistivity of OIP had a close relationship with the conductivity of transformer oil.

So for these reasons, the effect of temperature on conductivity of transformer oil would be discussed. The conductivity of liquid dielectric was divided into ionic conductivity and electrophoresis conductivity according to the charge carriers. The ions were activated by the thermal excitation. Then the ions were deviated from the stable position and activated and migrated due to thermal vibration energy of ions over the potential barrier of adjacent molecule. The conductivity of transformer oil mainly depended on impurity ions with small mobility at room temperature. Meanwhile, the activation energy u_a decreased Δu_a when the ions were dissociated from molecule under the external electric field. Thus, the conductivity of oil was calculated as equation (1)

$$\gamma = j/E = n_0 q\mu, \tag{1}$$

where j denotes current density, E denotes external electric field strength, q denotes charge of ion, μ denotes mobility of ion, n_0 denotes density of ion in liquid dielectric.

According to Pool–Frenkel effect, the molecular dissociation activation energy would reduce Δu_a under the electric field, and it could be calculated as follows: $\Delta u_a = \sqrt{q^3E/\pi\varepsilon\varepsilon_0}$.

So, the μ and n_0 under external electric field were calculated as equations (2) and (3).

$$n_0 = A_0 \exp((\Delta u_a - u_a)/2kT), \tag{2}$$

$$\mu = (q\delta^2 v/6kT)\exp(-u_0/kT), \tag{3}$$

where A_0 denotes constant, k denote Boltzmann constant, T denotes thermodynamic temperature, u_a denotes activation energy, ε is permittivity of liquid dielectric, ε_0 denotes Permittivity of vacuum, δ *is* average distance of ion transition, u_0 is potential barrier of ion, v is vibration frequency of ion.

The density of ion in transformer oil gradually increased and the mobility of ion gradually accelerated as temperature increased. It could be calculated from the equations (2) and (3).

So the volume resistivity could be calculated as equation (4)

$$\rho_1 = (6kT/A_0q^2\delta^2 v)\exp((2u_0 + u_a - \sqrt{q^3E/\pi\varepsilon\varepsilon_0})/2kT). \tag{4}$$

Equation (4) could be written as

$$\rho = Ae^{\frac{B-C\sqrt{E}}{T}}, \tag{5}$$

where $A = 6kT/A_0q^2\delta^2 v$, $B = (2u_0 + u_a)/2k$, $C = \sqrt{q^3/\pi\varepsilon\varepsilon_0}/2k$.

So the equation (5) was equal to

$$\ln\rho = \ln A + B/T - C\sqrt{E}/T$$

$\partial \ln\rho/\partial T = -(B - C\sqrt{E})/T^2 < 0$, so, the volume resistivity decreased as temperature increased. $\partial \ln\rho/\partial E = -0.5C/T^2E^{-0.5} < 0$, thus, the volume resistivity decreased as electric field strength increased.

According to the equation (5), the volume resistivity was reduced under the influence of temperature and electric field strength.

The OIP surface conductivity was related to the characteristics of OIP, such as temperature, humidity and surface topography. Although the pressboard was disposed through the vacuum drying and impregnated, there was less water in

the OIP. The water appeared as degraded product when the pressboard was degraded by the high temperature. The water migrated from the OIP into transformer oil as the temperature increased. A portion of water dissolved into the oil, and the other part of water existed in the oil as suspended water. The suspended water exhibited directional movement along the electric field, and formed the electrophoresis conductivity of transformer oil.

We assumed that the suspended water existed as spherical shape. The potential of suspended water relative to oil was U_0, and the radius of sphere was r. Thus, the charge of suspended water was calculated as equation: $q = 4\pi\varepsilon\varepsilon_0 r U_0$. So, the electric field force under external electric field E was calculated as equation (6)

$$F = qE = 4\pi\varepsilon\varepsilon_0 r U_0 E. \tag{6}$$

The suspended water was subjected to the friction when it moved in the oil. The friction was calculated as equation (7) according to Stokes law.

$$F' = 6\pi r\eta v, \tag{7}$$

where F' denote friction, v denote velocity of water suspend particles, η denote viscosity of transformer oil.

If $F' = F$, the suspended water moved at the constant velocity. Thus, the mobility of suspended water was calculated as equation (8)

$$\mu = v/E = q/6\pi r\eta = 2\varepsilon\varepsilon_0 U_0/3\eta. \tag{8}$$

So, the electrophoresis resistivity of oil was calculated as equation (9)

$$\rho_2 = 3\eta/8\pi r n_0 \varepsilon^2 \varepsilon_0^2 U_0^2 \tag{9}$$

From the equation (9), it indicated that the mobility of suspend water and the electrophoresis conductivity were influenced by ε, n_0, and η. These parameters were affected by the temperature. Therefore, it could be deduced that the conductivity was seriously influenced by the temperature. In OIP insulation systems the effect of temperature was usually twofold. An increase in temperature would result in increasing in conductivity and amplitude of PD during the process of creepage discharge.

Therefore, the magnitude and density of charge carriers increased due to the higher surface and volume conductivity with higher temperature in OIP under applied voltage. The results show that under the same electric field strength, the conduction current of the higher temperature OIP was greater than that at low temperature. As the temperature increased, the charge carriers were more easily accumulated and quickly moved in direction of electric field. The residual charge carriers were more easily dissipated after once discharging. Thus, the times of LAD gradually decreased and amplitude of LAD increased with higher temperature at each stage. However, the times of HAD gradually increased at each stage of creepage discharge.

At present, this study investigated the creepage discharge characteristics of OIP insulation under the action of power frequency (50 Hz) AC and DC voltage, and achieved some results. There are few studies on the ratio of combined voltage and the creepgae discharge characteristics under the voltage type of harmonic voltage components of other frequencies. In the follow-up studies, the voltage effects of the AC voltage component and the DC voltage component of different ratios should be discussed, and the harmonic voltage components of other frequencies should be included, so that the insulation performance of the OIP insulation under the combined AC–DC voltage can be more comprehensively evaluated. This can be closer to the actual working conditions of the converter transformer, and some works have been carried out.

4. Conclusions

Due to the unique operating characteristics of the valve side winding of the converter transformer, it can withstand the combined effects of AC and DC voltages and thermal fields. The effect of temperature on creepage discharge characteristics of OIP was studied in laboratory. The PDIV and CDFV decreased linearly as the temperature increased under the same combined AC–DC voltage. The LAD appeared in 'hump' and moved to the direction of higher discharge magnitude. The analysis indicated that the surface and volume resistivity of OIP decreased exponentially with higher temperature, resulting in the charge carriers easily accumulating and quickly migrating directional movement along the electric field ahead of discharging. The residual charge carriers were more easily dissipated after discharging. Therefore, the times of LAD decreased and amplitude of LAD increased with higher temperature at each stage. Meanwhile, the times of HAD gradually increased at each stage of creepage discharge with higher temperature. The energy of HAD seriously destroyed surface of OIP, resulting in shortening the time between discharge inception and breakdown, accelerating the development of creepage discharge.

Acknowledgments

This work is supported by the Natural Science Foundation of Qinghai Province (No. 2016-ZJ-925Q) and Chinese National Programs for Fundamental Research (No. 2011CB209400).

References

[1] Zhang Y B *et al* 2010 *High Voltage Eng.* **36** 255 (in Chinese)
[2] Maruvada P S 2008 800kV HVDC transmission systems *Proc. 2008 IEEE/PES Transmission and Distribution Conf. and Exposition* (Chicago: IEEE)
[3] Li H Q *et al* 2014 *IEEE Trans. Dielectr. Electr. Insul.* **21** 1851
[4] Whitehead J B 1931 *Trans. Am. Inst. Electr. Eng.* **50** 692
[5] Beroual A *et al* 1998 *IEEE Electr. Insul. Mag.* **14** 6
[6] Sajan J S, Dwarakanath K and Moorching S N 1998 Comparative evaluation of dielectric strength of paper-oil insulation under ac, dc, combined, composite ac/dc and impulse voltages *Proc. 1998 Annual Report Conf. on Electrical Insulation and Dielectric Phenomena* (Atlanta: IEEE)

[7] Tobazcon R 1994 *IEEE Trans. Dielectr. Electr. Insul.* **1** 1132
[8] Kelley E F and Hebner R E 1981 *IEEE Trans. Electr. Insul.* **EI-16** 297
[9] Cross J D 1982 *IEEE Trans. Electr. Insul.* **EI-17** 493
[10] Devins J C and Rzad S J 1982 *IEEE Trans. Electr. Insul.* **EI-17** 512
[11] Wechsler K and Riccitiello M 1961 *Trans. Am. Inst. Electr. Eng.* III **80** 365
[12] Taylor R J 1977 *Proc. Inst. Electr. Eng.* **124** 899
[13] Takahashi E *et al* 1976 *IEEE Trans. Power Appar. Syst.* **95** 411
[14] Anker M U 1983 *IEEE Trans. Power Appar. Syst.* **PAS-102** 3796
[15] Okubo H *et al* 1987 *IEEE Trans. Power Deliv.* **2** 126
[16] Raghuveer M R *et al* 1990 *IEEE Trans. Electr. Insul.* **25** 341
[17] Tulasi Ram S S, Kamaraju M and Singh B P 1994 Flashover behaviour of converter transformer insulation subjected to superimposed ac and dc voltages *Proc. IEEE Conf. on Electrical Insulation and Dielectric Phenomena* (Arlington: IEEE)
[18] Wang H *et al* 2010 *High Voltage Eng.* **36** 884 (in Chinese)
[19] Wang W *et al* 2011 *High Voltage Eng.* **37** 1924 (in Chinese)
[20] Qi B, Wei Z and Li C R 2016 *IEEE Trans. Dielectr. Electr. Insul.* **23** 237
[21] Jang K *et al* 2016 Nano SiO_2/epoxy coating effect on creepage discharge characteristics in oil/pressboard composite insulation system *Proc. 2016 IEEE Int. Conf. on Dielectrics* (Montpellier: IEEE)
[22] Dai J, Wang Z D and Jarman P 2010 *IEEE Trans. Dielectr. Electr. Insul.* **17** 1327
[23] Kurachi M *et al* 2017 Dielectric properties and creepage discharge of epoxy/silica nanocomposite in mineral oil *Proc. IEEE 19th Int. Conf. on Dielectric Liquids* (Manchester: IEEE)
[24] Jang K *et al* 2017 *IEEJ Trans. Fundam. Mater.* **137** 113
[25] Dai Q M *et al* 2017 *Trans. China Electrotech. Soc.* **32** 181 (in Chinese)
[26] Chi M H *et al* 2015 *Proc. CSEE* **35** 1524 (in Chinese)
[27] Yang L J *et al* 2016 *IEEE Trans. Dielectr. Electr. Insul.* **23** 1393
[28] Chen Q G *et al* 2018 *Energies* **11** 2271
[29] Du B X *et al* 2018 Numerical simulation of electric field distribution along the DC-GIL spacer with SF6/N2 mixture *Proc. 2nd IEEE Int. Conf. on Dielectrics* (Budapest: IEEE)
[30] Liao R J *et al* 2016 Effect of temperature on 2-furfural partitioning in the oil-paper system of power transformers *Proc. 2016 Electrical Insulation Conf.* (Montreal: IEEE)
[31] Wu G N, Zhong X and Bao J K 2015 *High Voltage Eng.* **41** 4081 (in Chinese)
[32] Baral A and Chakravorti S 2016 *IEEE Trans. Dielectr. Electr. Insul.* **23** 2462
[33] Jin F B *et al* 2018 Effects of temperature on characteristics of creepage discharge in oil-impregnated pressboard insulation under combined AC–DC voltage *Proc. 12th IEEE Int. Conf. on the Properties and Applications of Dielectric Materials Xi'an (Piscataway, NJ)* (IEEE)
[34] Zhou Y X *et al* 2015 *IEEE Trans. Dielectr. Electr. Insul.* **22** 2737
[35] Zhou Y X *et al* 2013 Influence of temperature on developing process of surface flashover in oil-paper insulation under combined AC–DC voltage *Proc. 2013 Annual Report Conf. on Electrical Insulation and Dielectric Phenomena* (Shenzhen: IEEE)
[36] Zhou Y X *et al* 2013 Surface flashover characteristics of oil-paper insulation under combined AC-DC voltage *Proc. 2013 IEEE Int. Conf. on Solid Dielectrics* (Bologna: IEEE)
[37] IEC 60270-2000 2000 High-voltage test techniques-Partial discharge measurements *Commission Elctrorechnique Int. (CEI) Int. Electrotechnical Commission (IEC)* (Geneva: CEI IEC)
[38] IEC 61378-2-2001 2001 Convertor transformers: 2. Transformers for HVDC applications *Commission Elctrorechnique Int. (CEI) Int. Electrotechnical Commission (IEC)* (Geneva: CEI IEC)